

A Spatial Filter for the Removal of Striping Artifacts in Digital Elevation Models

Marco Albani and Brian Klinkenberg

Abstract

Elongated topographic artifacts, such as the striping production artifacts described for USGS 7.5-minute DEMs, can result in globally biased estimates of slope and aspect. As such, developing methods to reduce these artifacts and their resulting biases is important. This study presents an algorithm for the mitigation of these artifacts, using Terrain Resource Information Management (TRIM) digital elevation models (DEMs) of the Fort St. John Forest District, in British Columbia, Canada, as the test bed. The algorithm uses a theoretical error model, where elevation measurement errors are assumed to be autocorrelated along the collection lines of the photogrammetric model, and takes advantage of the entry order of DEM points to apply a sequence of spatial filters to the elevation. A probability function is used to constrain the elevation changes to an acceptable range. The algorithm is effective in mitigating the artifacts' effects on slope and aspect while preserving the original topographic detail.

Introduction

Digital elevation models (DEMs), a gridded numerical representation of terrain elevation, are used in an increasingly wide range of analytical applications (Weibel and Heller, 1991; Pike, 2000). As DEM applications become more widespread, so does concern about the quality of the available elevation data and the propagation of DEM errors through the analyses. It is now well documented that the results of most DEM-based quantitative operations are influenced not only by the magnitude but also by the spatial distribution of elevation errors (Fisher, 1991; Lee *et al.*, 1992; Bolstad and Stowe, 1994; Hunter and Goodchild, 1997; Fisher, 1998; Heuvelink, 1998). However, most DEM producers, like the United States Geological Survey or the British Ordnance Survey, report only the average magnitude of DEM errors as the root-mean-square error (RMSE), which does not provide information on systematic bias (Li, 1988) nor on the spatial patterns of the DEM errors (Guth, 1992).

Artifacts, i.e., spatially structured errors of a systematic nature, are often associated with the production of DEMs. The interpolation of DEMs from contour line maps, for example, can produce several kinds of artifacts (Carrara *et al.*, 1997), an example of which is that of contour line "ghosts" in USGS Level 2 DEMs (Guth, 1999). Different kinds of artifacts are associated with DEMs produced directly from photogrammetric models (Kok and Rangayyan, 1987). In particular, striping artifacts have been described for level 1 USGS

DEMs (Brunson and Olsen, 1978; Hassan, 1988; Klinkenberg and Goodchild, 1992; Brown and Bara, 1994; Garbrecht and Starks, 1995; Oimoen, 2000). Striping artifacts are also found in the Terrain Resource Information Management (TRIM) digital map product of the Province of British Columbia (BC), Canada. In this paper we describe an algorithm that mitigates these artifacts by taking advantage of the specific structure of the TRIM product. While the methodology described below was applied to BC TRIM data, it could be applied to any digital elevation data collected using a profiling technique (Petrie, 1990).

Production Artifacts as Spatially Structured Elevation Error

In December of 1996, the Ministry of Environment, Land, and Parks (MoELP) of the Province of British Columbia, Canada, announced the completion of the digital production of 7027 1:20,000-scale Terrain Resource Information Management (TRIM) maps that cover the entire province (GDBC, 1999). The TRIM product contains digital elevation data that are designed to produce triangulated irregular networks (TINs). TRIM elevation data is organized into two vector files: a file of elevation (mass) points, hereafter referred to as the DEM file, and a file of break lines (GDBC, 1992). Elevation points, typically collected using a semi-automated profiling technique, are distributed on a semi-regular grid spaced between 75 and 100 m apart, and are collected in sequence along profiles generally oriented north-south (GDBC, 1992). As a result of their collection methodology, groups of sequentially measured elevation points, hereafter referred to as "collection lines," are generally recognizable. As one might expect, elevation values within collection lines have a higher degree of spatial autocorrelation than do elevation values between collection lines, especially in areas with limited topographic variability. This produces topographic artifacts manifested by "stripes" or "ridges" aligned with the collection lines. These collection line artifacts are particularly evident in analytical hill-shading images or in aspect maps generated from the TRIM data source. Oimoen (2000) provides several examples of similar problems encountered in USGS DEMs.

The authors encountered collection line artifacts while working with TRIM digital elevation models on a landscape ecology investigation in the area of the Halfway and Peace River watersheds in northeastern British Columbia. Sixty-three 1:20,000-scale map sheets were made available for digital terrain analysis by the Fort St. John Forest District, British Columbia Ministry of Forests. Several of these, when converted to 30-m-resolution raster DEMs, showed evidence of "stripes" aligned with the collection lines of the DEM points. Their perfect alignment with the collection lines,

M. Albani was with the Department of Forest Sciences, University of British Columbia, 2424 Main Mall, Vancouver, BC V6T 1Z4, Canada; he is presently with the Department of Organismic & Evolutionary Biology, Harvard University, HUH 22 Divinity Avenue, Cambridge, MA 02138 (malbani@fas.harvard.edu).

B. Klinkenberg is with the Department of Geography, University of British Columbia, 1984 West Mall, Vancouver, BC V6T 1Z2, Canada.

Photogrammetric Engineering & Remote Sensing
Vol. 69, No. 7, July 2003, pp. 755-765.

0099-1112/03/6907-755\$3.00/0

© 2003 American Society for Photogrammetry
and Remote Sensing

and the fact that the “stripes” do not conform to the topographic patterns delineated by watercourses in the TRIM line files, made them recognizable as systematic errors (artifacts) and not authentic topographic features (Figure 1). This was confirmed by field and aerial photograph observation for one of the map sheets and by visual inspection of Landsat 5 satellite images for the rest of the map sheets. Similar artifacts have been described in USGS 7.5-minute DEMs produced with the manual profiling method (Garbrecht and Starks, 1995; Garbrecht and Martz, 2000).

Collection line artifacts can be assumed to be the consequence of a specific spatial distribution of elevation errors. For the stripes to appear, part of the elevation error must have high autocorrelation in the direction of the collection lines, and low autocorrelation in the orthogonal direction. As stated by Oimoen (2000, quoting Brunson and Olsen (1978)), “data thus collected” (by manual profiling) “reflect ‘... a systematic operator tendency to profile above ground while scanning downhill and underground while scanning uphill.’” We feel that this autocorrelational effect is actually widespread throughout a DEM, but that it is most obvious on hillslopes because of the herringbone pattern that results. The collection line artifacts are similar to the scan-line noise (Crippen, 1989) or “striping” (Pan and Chang, 1992) of satellite imagery, and generally conform to the expected error structure of any measurement that is performed in sequence. We propose the following error model for DEM data points:

$$Z(x,j) = z(x) + k(j) + e \quad (1)$$

where Z is the measured elevation at the point x in geographical space and position j in a collection line, z is the real (actual) elevation at the same point, k is an error term which is only a function of the position (j) on the collection line, and e is a residual error term. Note that, because we have only one measure of Z at each (x,j) , it is not possible to estimate k at a given j without making assumptions on the spatial distribution of k and z . However, only three realistic assumptions are necessary to produce the collection lines artifacts:

- k must be autocorrelated along j ,
- k be larger than e , and
- z must be autocorrelated in x .

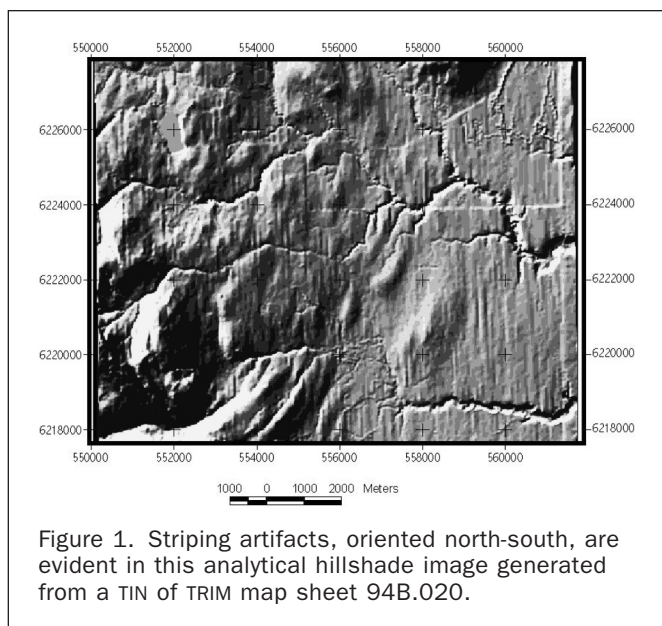


Figure 1. Striping artifacts, oriented north-south, are evident in this analytical hillshade image generated from a TIN of TRIM map sheet 94B.020.

The presence of collection-line artifacts does not indicate a violation of the accuracy standards for the TRIM map product. The accuracy specification of the TRIM product for spot elevation points is a Linear Mapping Accuracy Standard (LMAS) for the elevation of less than 5 meters, corresponding to a maximum RMSE of 3 meters (GDBC, 1992). It is possible to assume that the distribution of $k + e$ meets the TRIM mapping accuracy standards, with variance lower than the square of the maximum acceptable root-mean-square error (RMSE): i.e.,

$$\text{VAR}(k + e) \leq \text{RMSE}(Z)^2 \quad (2)$$

When the DEM points are irregularly distributed, the specifications for the spacing of the points are expressed in terms of minimum point density, with an average spacing of 100 m in areas of slope less than 25°, and of 75 m in areas of slope greater than 25° (GDBC, 1992). As a consequence, the maximum acceptable RMSE of the slope measured between two independent points is 6 percent when the points are 100 meters apart, which is sufficient to create artifacts in low relief areas.

The spatial distribution of elevation errors influences local operations that are performed on DEMs (Lee *et al.*, 1992; Hunter and Goodchild, 1997; Fisher, 1998; Heuvelink, 1998). Terrain parameters that are based on the first or second derivative of the DEM surface, such as slope, aspect, and surface curvature, are particularly influenced by the spatial autocorrelation of DEM errors. In DEMs where the spatial autocorrelation of errors is positive and isotropic, the errors introduce a local bias in elevation but have little influence on overall surface shape. Conversely, errors that have negative or no spatial autocorrelation can greatly influence the local shape of the surface, introducing the most noise in the estimate of terrain parameters (Hunter and Goodchild, 1997; Heuvelink, 1998). Collection line artifacts have strong anisotropy in the autocorrelation of the error, and influence parameter estimation differently than do isotropic autocorrelated errors. The error influence on slope depends on the orientation of the collection lines relative to the orientation of the terrain surface. In the case of the TRIM data—as it would be for most data collected using a profiling method—the collection line orientation is mostly the same for the entire map sheet; therefore, aspect estimates will not only be erroneous locally, but also globally biased toward the direction orthogonal to the collection lines. Collection line artifacts will also negatively affect the parameterization of drainage features, similar to the effect associated with striping patterns observed in some USGS 7.5-minute DEMs (Garbrecht and Martz, 2000; Oimoen, 2000). For these reasons and more, it is desirable to mitigate line collection artifacts prior to performing local operations on the DEM data.

The Filter Employed: Line-Based Cross-Smoothing.

Fortunately, because of their specific structure, collection line artifacts are easier to identify and target for removal than are less structured errors. The artifacts can be removed using a filter that targets the component of the elevation signal that is autocorrelated along the direction of the profile (j), but has no autocorrelation in x (Equation 1), which is equivalent to targeting that part of the elevation signal that has low frequency along the collection lines and high frequency in the orthogonal direction. This is the approach proposed by Crippen (1989) for the cosmetic removal of scan-line noise in Landsat images, and more recently by Oimoen (2000) for the removal of striping artifacts from USGS 7.5-minute DEMs. Both Crippen’s (1989) and Oimoen’s (2000) methods operate on regular grids, alternatively fil-

tering along rows and columns. In the case of TRIM DEMs, the original elevation points were not collected on a regular grid, and, while it is possible to apply Oimoen's (2000) method to an interpolated grid, better results can be obtained by operating directly on the original data, if the collection lines can be identified, as they can be in the TRIM point file from the relative order of the elevation points. To this purpose we have devised a specific filtering algorithm, called line-based cross-smoothing. This algorithm was written as a series of functions in the S-plus command line language, taking advantage of the matrix operations of that language. The numerical values of the parameters used in the algorithm are summarized in Table 1; the general structure of the algorithm described below is presented in Figure 2.

Stage 1: Identification of the Collection Lines

The first step of the algorithm is to identify the collection lines. Elevation points' assignment to individual collection lines is based on their order in the database, their relative distance in UTM coordinates, and the orientation of the segments defined by each sequence of two points. A sequence of points in the database is organized into a unique collection line if the Manhattan distance (city-block or absolute distance; see Dillon and Goldstein (1984), p. 162, for an explanation) between two consecutive points is lower than a specified threshold, and the difference in azimuth between two consecutive segments is within a specified threshold. The Manhattan distance was chosen because its calculation is faster than that of the Euclidean distance and it performed equally well in tests. This step requires the definition of three parameters: $XMAX$ and $YMAX$, the maximum distances in the x and y directions between two consecutive points before a line is broken, and $AMAX$, the maximum change of azimuth allowed between two consecutive segments before a line is broken. The values of the parameters are chosen to avoid the interruption of the line when there are slight changes of direction, or when one or two points are missing from the semi-regular sampling scheme, as happens when the elevation point would fall over a small lake, wetland, or other feature that is represented in the break-lines file. In our implementation we used a value of 250 m for $XMAX$ and $YMAX$, and a value of 15° for $AMAX$, with excellent results in line recognition.

Stage 2: Filtering of the Artifacts

Once the collection lines have been identified, the striping is filtered out using a procedure conceptually similar to that of Crippen (1989) and Oimoen (2000), but with necessary modifications because those methods were designed for regular grids, while the data set we have consists of an irregular structure. The filtering algorithm consists of six steps:

- (1) A surface grid is interpolated around each collection line. The grid is aligned with the collection line, so that it is possible to apply directional filters that are orthogonal to the collection line. This step is necessary in order to separate x from y as much as possible (Equation 1), by considering only the variation of Z in the direction orthogonal to j . The grid nodes are spaced to minimize the average distance from each original point to a node in the grid. The algorithm uses the *interp* function of S-plus (MathSoft, 2000) for the interpolation, an interpolator for irregular data points based on Akima's (1978) work. The resolution of the grid, RES , is the first parameter in this step. The grid should be fine enough to allow for a smooth description of the interpolated surface, but a very fine grid is inefficient because only the original points are eventually retained. We obtained satisfactory results in speed and precision with a grid resolution of 20 m. The other parameters are the number of points used for the interpolation of each node, $NPSINT$, and the

TABLE 1. PARAMETERS USED IN THE IMPLEMENTATION OF THE LINE-BASED CROSS-SMOOTHING FILTER (SEE TEXT FOR EXPLANATION)

Parameter	Value
$XMAX, YMAX$	250 m
$AMAX$	15°
RES	20 m
$NPSINT$	6
WID	15
$MINPS$	9
$NPOINTS$	7
p_1	0.997
p_2	0.850

width of the grid in the direction orthogonal to the collection line. The width of the grid should be chosen so that it can accommodate the kernel of the filter described in the next step.

- (2) A mean low-pass filter is applied to the grid in the direction orthogonal to the collection line, with a fixed kernel of size $1 \times WID$. The product of WID and RES gives the width of the kernel in map units, and should be calibrated to fit the spacing of the collection lines, so that the kernel spans a few collection lines, keeping in mind that the spacing of the collection lines is generally not constant over a TRIM map sheet. In our case a WID of 15, giving a 300-m kernel, produced the best results.
- (3) Because the filter of Step 2 operated on an interpolated regular grid, it is now necessary to assign a filtered value to each original point in the collection line. This is done using inverse distance weight (IDW) interpolation (Lam, 1983) of the four nodes of the grid closest to each original elevation point.
- (4) The difference, R , between the original elevation value and the filtered value is recorded for every point. This residual value is considered to be composed of the sum of error k (assumed to have low frequency along the collection line) and hz (the high-frequency component of elevation in the direction orthogonal to the collection line): i.e.,

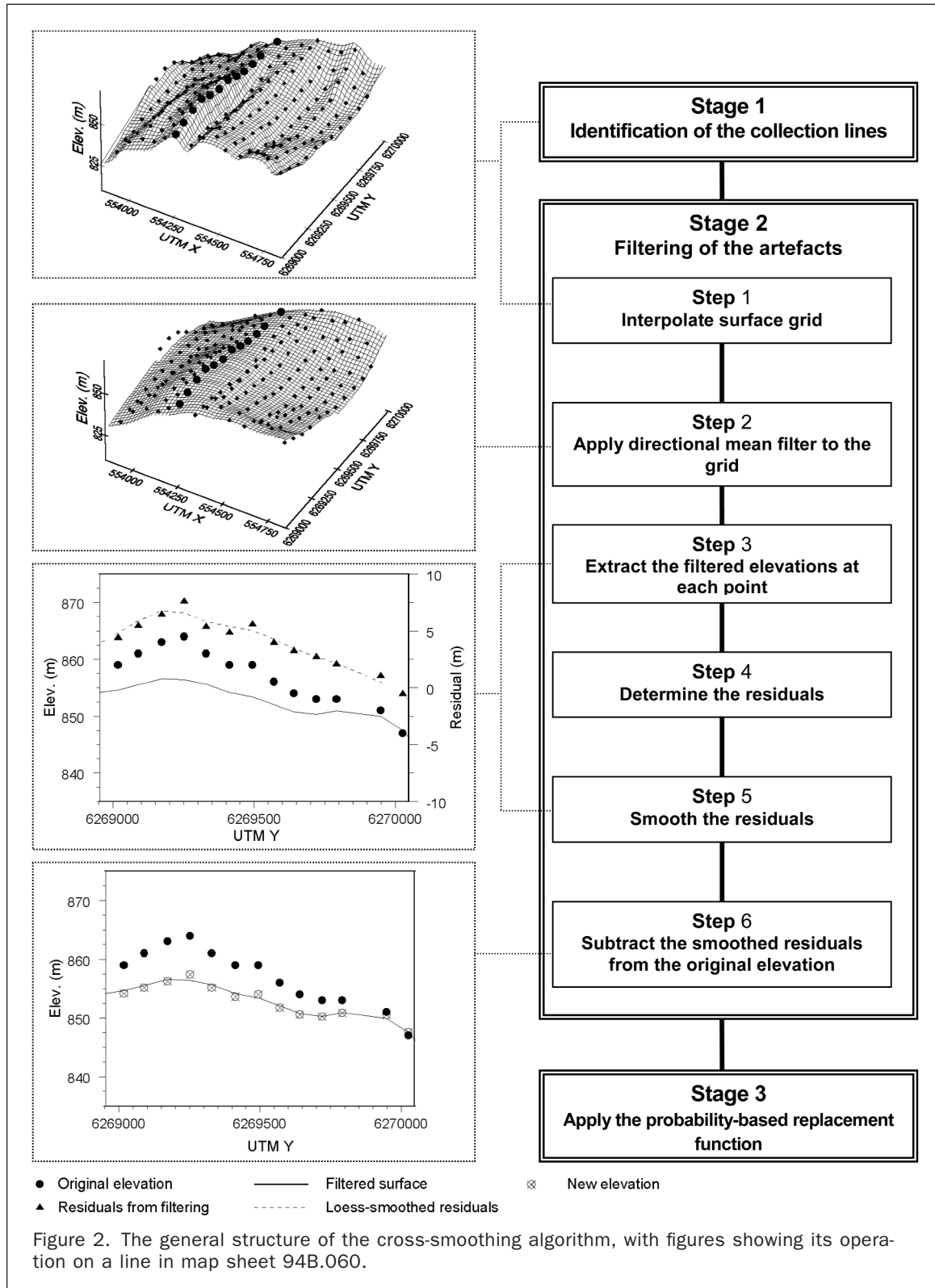
$$R \approx hz + k. \quad (3)$$

- (5) A loess interpolator, a localized regression function, is then applied to the R values along each collection line. The interpolator is used to separate k from hz , because hz is also assumed to have a high-frequency component along the collection line. The *loess* function of S-plus is used, using the distance of each point from the beginning of the collection line as the predictor variable. Only lines that have at least a minimum number of points (parameter $MINPS$, which we set to 9) are processed. A scale parameter for the loess function—the size of the kernel where the local regression is applied—is the span. In the S-plus *loess* function the span is specified as a fraction of the total number of points in the collection line. In our algorithm a different span is calculated for each individual collection line in order to ensure that the kernel always includes the same number of points ($NPOINTS$, set to 7 in our implementation). The *loess* function then operates as a low-pass mean filter with a fixed number of original points included in the kernel, but a variable span length, to account for the irregular nature of the distribution of TRIM elevation points. The loess interpolator was chosen because it allows for unevenly spaced points along the collection line, it does not require any specific assumption about the relation between k and the position on the collection line, and it is relatively robust and can be implemented even when collection lines are relatively short.
- (6) A new filtered elevation estimate FZ is then obtained by subtracting the loess interpolation result from the original measurement: i.e.,

$$FZ = Z - loess(R). \quad (4)$$

Stage 3: The Probability-Based Replacement Function

While the filter described above will work well in many cases, sometimes it can produce values of FZ that depart from



Z more than it would be reasonable to expect considering the assumed distribution of k . A probability-based replacement function can be used to constrain replacements of Z with FZ within an acceptable range. This function is based on the concept that the probability of FZ , representing a better estimate of the true elevation, decreases when the difference ΔZ (i.e., $\text{loess}(R)$) between FZ and Z exceeds cer-

tain thresholds, based on the mapping accuracy standards. In Equation 2 we assumed that the total error (line collection error plus spatially unstructured error) is within the mapping accuracy standards, normally distributed with zero mean. This later assumption is not always justified in real DEMs (Monckton, 1994), but it is the assumption behind the use of the RMSE as a single descriptor of DEM accu-

racy (Li, 1988). Based on this assumption, it is then possible to calculate the probability $p(\Delta Z)$ that the difference between the measured elevation and the unknown real elevation would be equal to or lower than ΔZ .

Where $p(\Delta Z)$ is lower than a certain threshold, it is reasonable to retain the original Z value as a better estimate of the real z . Instead of using a single threshold, a "fuzzy" threshold can be employed. The fuzzy replacement function is defined by two probability levels p_1 and p_2 . The first probability, p_1 , is the one above which the filtered value substitutes for the original value. The second probability p_2 is the one below which the original elevation value is maintained. At intermediate probabilities, the new elevation NZ is calculated as a weighted average of the two possible elevations: i.e.,

$$NZ = (1 - a)Z + aFZ$$

where

$$a = \begin{cases} 1 & \text{for } p(\Delta Z) > p_1 \\ \frac{p(\Delta Z) - p_2}{p_1 - p_2} & \text{for } p_2 \leq p(\Delta Z) \leq p_1 \\ 0 & \text{for } p(\Delta Z) < p_2 \end{cases} \quad (5)$$

The choice of the thresholds determines the amount of variation that the filtering process is allowed to impose on the original data points. The fuzzy threshold allows for a smoother transition between filtered and non-filtered values in areas where the filtered values might depart gradually from the original values.

Implementation

The cross-smoothing algorithm described above, including the replacement function, was applied to all 63 available TRIM map sheets. For reasons of brevity, the results for only two map sheets, chosen among those most plagued by the line collection artifacts, are reported here (Table 2). These are the map sheets 94B.020 and 94B.060 in the British Columbia Geographic System of Mapping (GDBC, 1992). The number of points affected by the cross-smoothing is lower than the overall number of points because *RES* cannot be calculated at the edges of the DEM, where it is not possible to apply the orthogonal filter. *FZ* is also not calculated for any individual collection line that has a number of points with valid *RES* lower than the *MINPS* parameter, the minimum for the loess function to operate. For all of these points the original Z values are retained. The summary statistics for change are calculated only for those points where an *FZ* value was calculated (Table 2).

For this application p_2 was set to 0.850 and p_1 to 0.997, meaning that the original points were retained if the probability of having a larger change by measurement error was lower than 85 percent, while they were fully replaced by the filtered value only when this probability was higher than 99.7 percent. Given the maximum acceptable RMSE of TRIM files, the possible change for each point was then limited to a range of ± 4.37 m. In each map sheet the mean of the change is slightly positive (0.24 m for 94B.020 and 0.13 for 94B.060; see Table 2); that is, the cross-smoothed DEMs are slightly lower than the original ones. While very small compared to the original DEM precision of 1 meter, these changes in global mean are significantly different from the effect of hypothetical measurement error at every single point using the maps' accuracy standards: the hypothesis that $E(Z - FZ) = 0$ given $VAR(Z - FZ) = 2 RSME^2$ can be rejected with a confidence level $\alpha = 0.001$ (z test, $p < 0.001$) for each map sheet. The z test is used instead of the t test because the variance is known and not estimated from a sample.

It is revealing to look at the spatial distribution of the changes, represented in Figure 3 as the difference between the TIN-based raster DEMs obtained from the original and the filtered point files, as described in the next section. Fifty-meter elevation contours obtained from the cross-smoothed DEM are superimposed on the difference images so that it is possible to relate the filter interaction with the shape of land.

The filter performed quite well in reducing the auto-correlated noise along the collection lines in the flatter areas. However, the greatest elevation changes are mostly associated with areas of more complex topography. In the east-facing slopes at the western edge of map sheet 94B.020, the filter is generally lowering the elevation. This happens again in the northwest corner and in the eastern section of 94B.060. The explanation lies in the general north-south orientation of the collection lines. The wide-kernel low-pass orthogonal filter used in Step 2 of the algorithm will particularly affect slopes where the gradient direction is orthogonal to the collection lines. If the slope face is sufficiently wide and generally oriented as the collection line, the low-pass filter does not capture a high-frequency component along the collection line. The signal is then indistinguishable from autocorrelated noise, and is captured by the loess function in Step 5 of the cross-smoothing algorithm. Because in these area the slopes are convex, the filter effect is to lower the elevation.

Filter Effect on Slope and Aspect

The objective of applying the cross-smoothing filter to DEM data is to improve the description of the terrain shape, not

TABLE 2. SUMMARY STATISTICS OF THE DEMS ELEVATION POINTS AND THE EFFECTS OF CROSS-SMOOTHING: THE CHANGE HAS NON-ZERO MEAN

Map Sheet		94B.020	94B.060
NZ Points		21892	25175
N Points Modified		20818	22153
Original Z Values	Mean	831.72	767.26
	Standard Deviation	127.17	68.66
	Minimum [†]	658	595
	Maximum [†]	1372	960
Cross-Smoothed Z Values	Mean	831.48	767.15
	Standard Deviation	127.00	68.57
	Minimum	658.00	595.00
	Maximum	1372.00	958.09
Change (Original - Cross-Smoothed)	Mean*	0.24	0.13
	Standard Deviation	1.56	1.78

*Significantly different from 0, $p < 0.001$ (z test).

[†] The original values have a precision of 1 m.

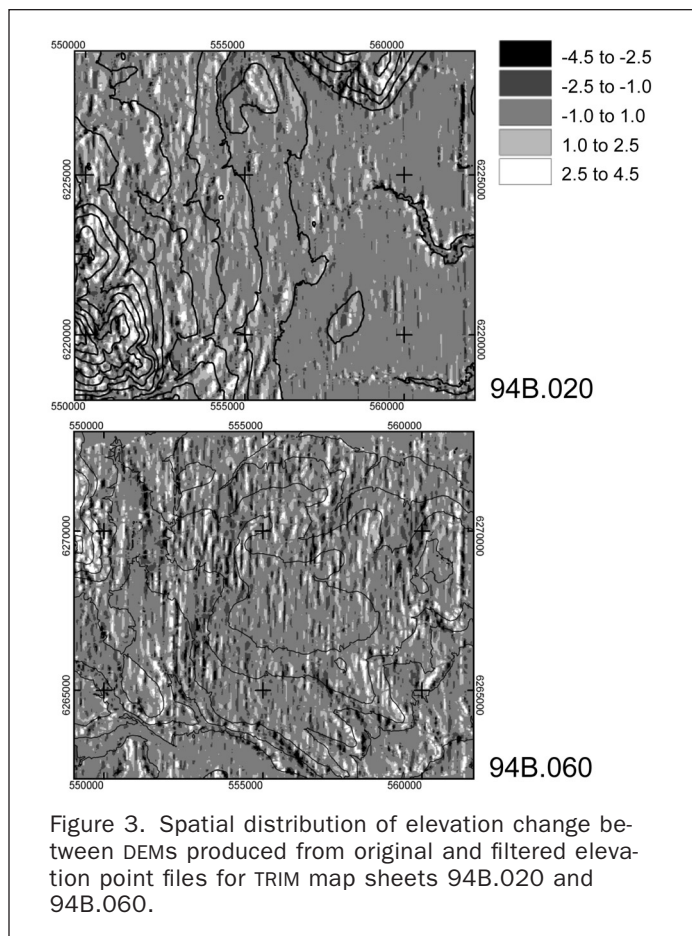


Figure 3. Spatial distribution of elevation change between DEMs produced from original and filtered elevation point files for TRIM map sheets 94B.020 and 94B.060.

to improve the DEM accuracy at any given point. To explore the effect of the filter on DEM-derived parameters, both the original and the filtered point files, together with the unaltered break-line files, were used to produce a TIN using the 3D Analyst extension of ESRI's ArcView GIS 3.2. Each TIN was then converted to a 30-m-resolution raster DEM using the default routine of Arc View 3D Analyst. Slope and aspect were then calculated from the raster DEMs using the LandSerf software by Wood (1996). The evaluation of the performance of the cross-smoothing filter is based only on how well it removes the collection-line artifacts, identified visually and subjectively as departures from the expected natural shape of the terrain. A proper quantitative estimate would require measures of slope and as-

pect from a source of greater accuracy, which was not available.

The calculation of slope and aspect from a gridded DEM is influenced by the algorithm used, with different algorithms generally producing different results (Skidmore, 1989; Jones, 1998). The quadratic regression model, proposed originally by Evans (1980) and implemented in the LandSerf software package by Wood (1996), has been proven to be the most precise method for these calculations (Florinsky, 1998; Jones, 1998). Wood's (1996) implementation of the algorithm in LandSerf, which is freely available for download on the Internet at the URL: <http://www.soi.city.ac.uk/~jwo/landserf/> (last accessed on 07 July 2002), has the advantage that it allows the user to calculate parameters (e.g., slope and aspect) with different window sizes, where the use of a wider window is akin to applying a quadratic smoothing filter to the DEM. In order to contrast the results of our filtering algorithm with those obtained by simply smoothing the DEM, slope and aspect were calculated from the two gridded DEMs using LandSerf with 3 by 3 and 5 by 5 windows, corresponding to windows of 90 by 90 and 150 by 150 meters. Both windows are wide enough to cover the signal from at least two different collection lines, given the general spacing of the lines in the TRIM data.

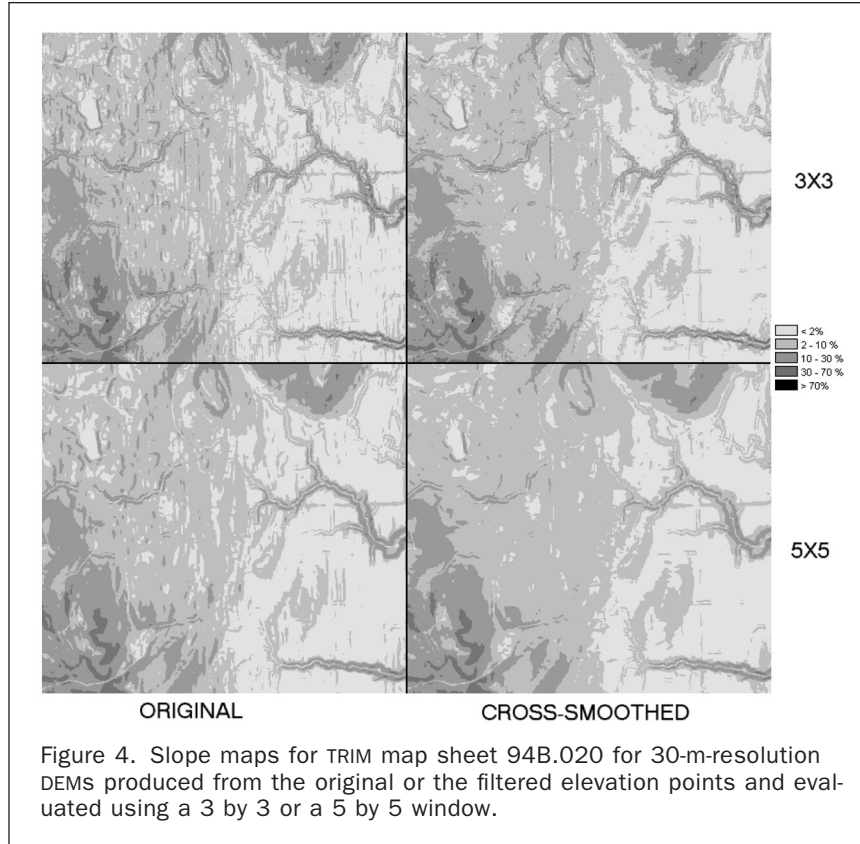
Slope data were then reclassified into five slope classes (Table 3). The class limits used are those relevant for an ecological classification of that area (Beckingham *et al.*, 1996).

Figures 4 and 5 show the slope maps obtained from the original and filtered DEMs with the two different window sizes. In both figures it is possible to observe the influence of the line collection artifacts on the slope estimate in the DEM obtained from the original TRIM data: vertical stripes of different slope class appear in areas of generally homogeneous slope. These artifact effects persist even when the slope is evaluated in a 5 by 5 window. The cross-smoothing filter is instead able to eliminate most of the artifact effects and retain the original detail, even when slopes are evaluated with a 3 by 3 window.

When compared to the results associated with the use of a 5 by 5 evaluation window, which eliminates the very steep slopes and greatly reduces the area of steep slopes, the areal distribution of slope classes is only slightly altered by the use of the cross-smoothing filter (Table 3, Figure 6). What is probably the most interesting effect is how the cross-smoothing filter alters the direction of the slopes, as evidenced in the aspect maps (Figures 7 and 8). Aspect is severely influenced by the collection line artifacts in both of the unfiltered map sheets, and again the cross-smoothing filter performs quite well in removing the artifacts' influence,

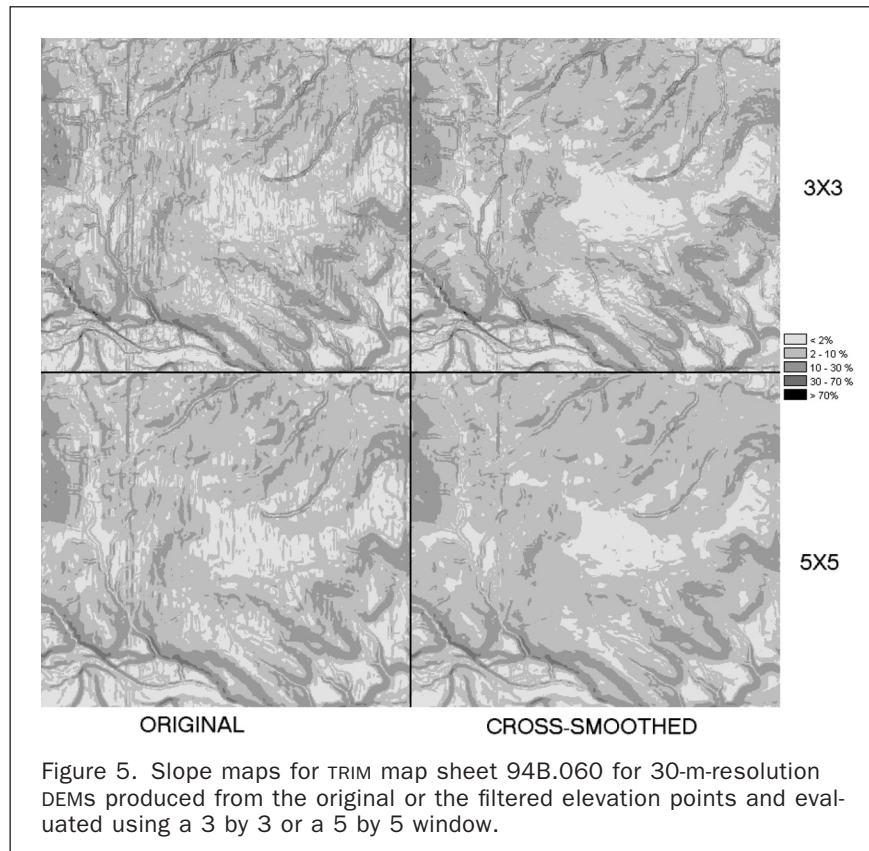
TABLE 3. AREAS (Ha) OF MAP SHEETS 94B.020 AND 94B.060 FALLING IN EACH SLOPE CLASS WHEN SLOPE IS CALCULATED FROM THE ORIGINAL AND THE CROSS-SMOOTHED DEM WITH WINDOW SIZES OF 3 BY 3 AND 5 BY 5. CROSS-SMOOTHING DOES NOT "SMOOTH OUT" THE STEEPER SLOPES

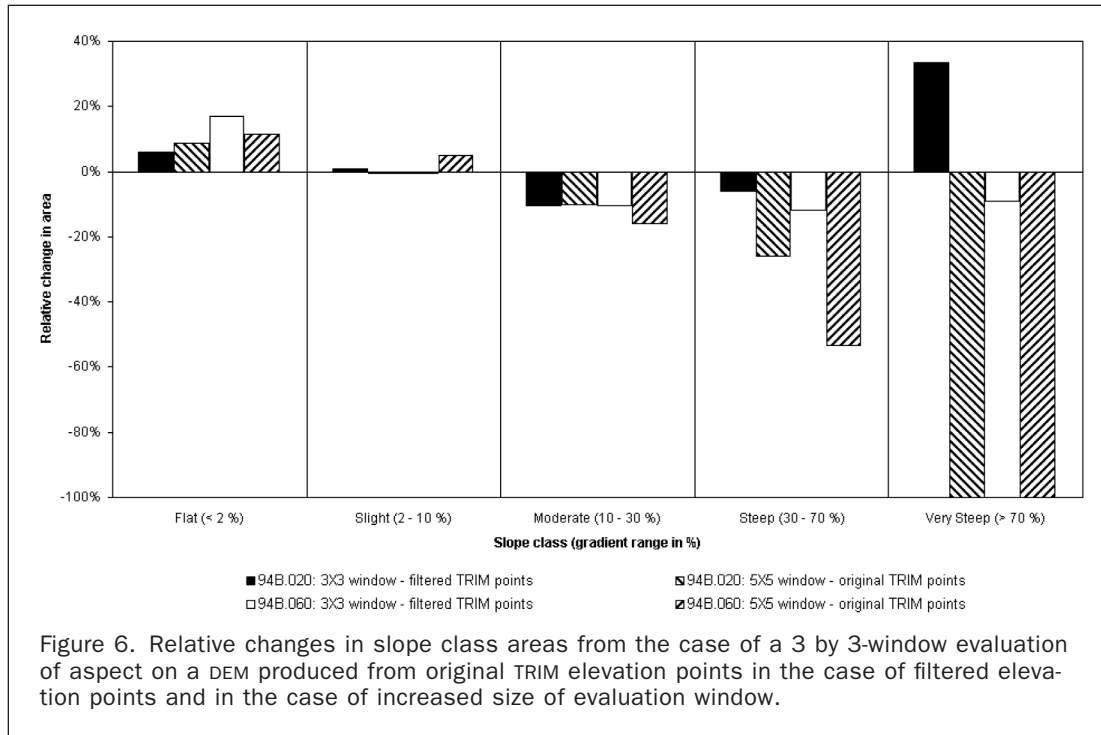
Slope Class	94B.020				94B.060			
	3 by 3 Window		5 by 5 Window		3 by 3 Window		5 by 5 Window	
	Original	Cross-Smoothed	Original	Cross-Smoothed	Original	Cross-Smoothed	Original	Cross-Smoothed
Flat (< 2%)	4113.3	4354.7	4479.6	3788.3	2276.4	2667.1	2541.1	1972.3
Slight (2 to 10%)	5970.7	6027.2	5945.4	7003.6	7233.4	7209.4	7591.4	8634.9
Moderate (10 to 30%)	2676.0	2394.3	2405.5	2061.3	3348.9	3002.5	2819.2	2358.5
Steep (30 to 70%)	271.8	255.4	201.5	178.8	172.4	152.2	80.3	66.3
Very Steep (> 70%)	0.3	0.4	0.0	0.0	1.0	0.9	0.0	0.0



even when the smaller window is used to evaluate aspect. Note, however, that there are some straight line features in both the aspect and slope maps that are not affected by the

cross-smoothing. These features correspond to roads, where the elevation measurements along the roads differ from the height of land interpolated from the point files. The road

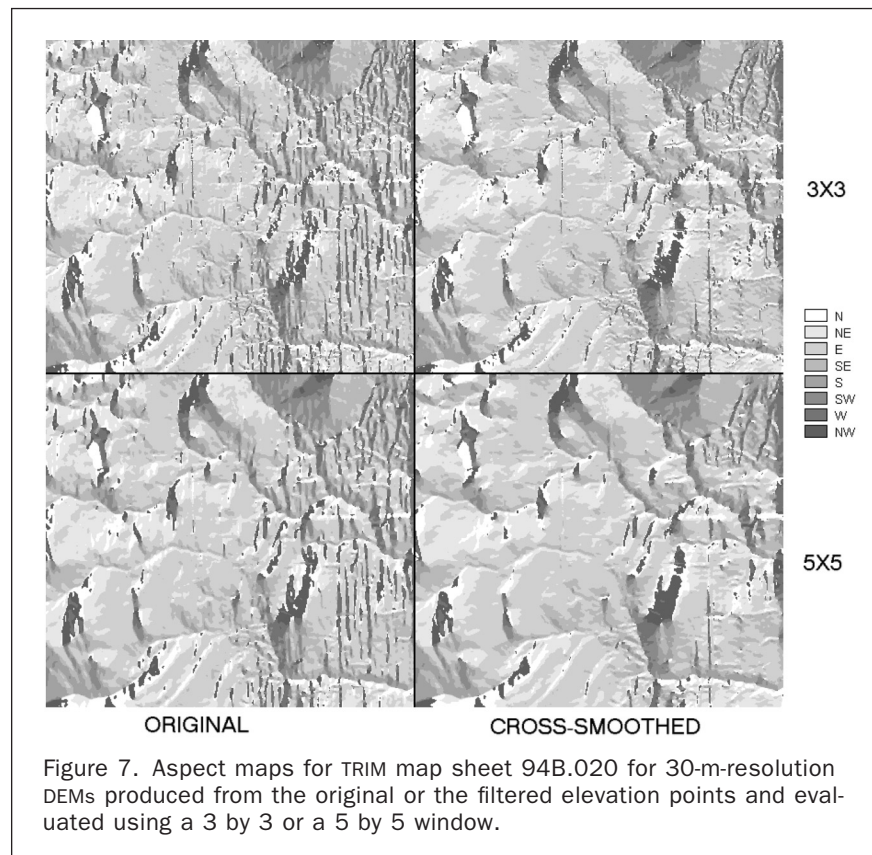




line-work comes from the TRIM break-lines files and was not subject to cross-smoothing.

The original DEMs show consistently less area in the north- and south-aspect classes than do the cross-smoothed

DEM (Table 4, Figure 9). This is to be expected, considering the general north-south direction of the striping artifacts, which create spurious east- and west-facing slopes that are eliminated by the cross-smoothing filter.



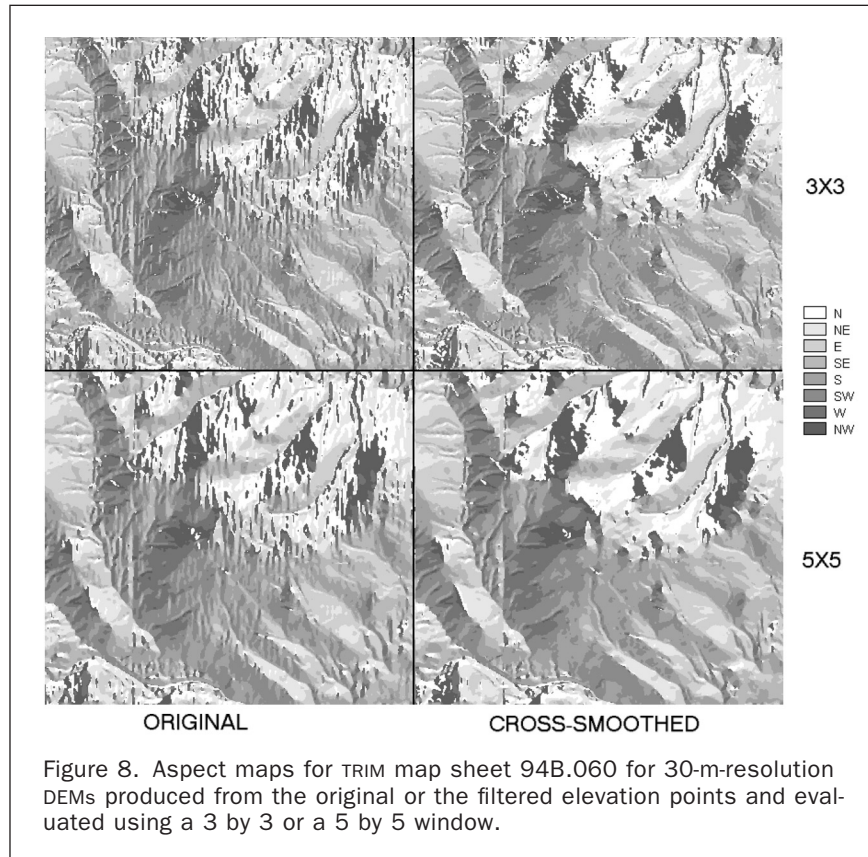


Figure 8. Aspect maps for TRIM map sheet 94B.060 for 30-m-resolution DEMs produced from the original or the filtered elevation points and evaluated using a 3 by 3 or a 5 by 5 window.

Conclusions

Collection-line artifacts, like scan-line noise in satellite images (Crippen, 1989), are a form of systematic error that is potentially more disruptive than its magnitude would indicate. Because of their high level of spatial structure, these artifacts greatly influence the estimate of local topographic parameters computed from a DEM in areas of generally low relief, and are likely to adversely affect any of the several possible subsequent GIS applications based on these parameters.

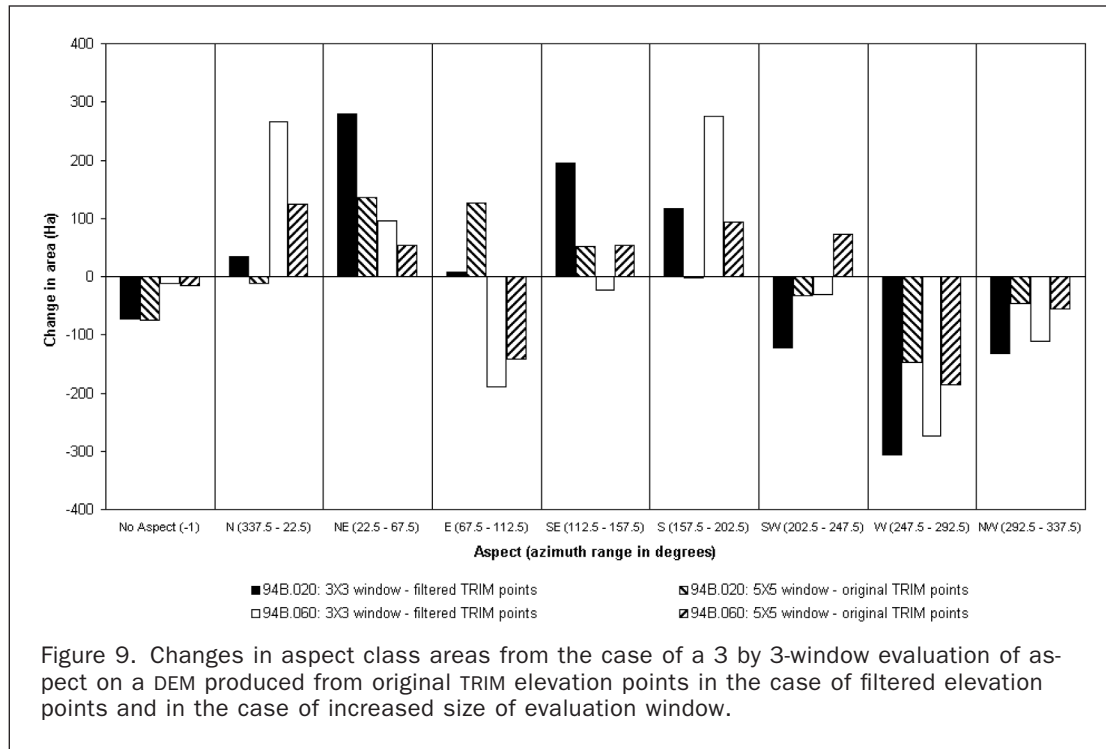
The line-based cross-smoothing algorithm described herein is based on a method previously employed for the cosmetic removal of similar systematic errors in Landsat images (Crippen, 1989). It was modified and applied to TRIM DEMs and has proven to satisfactorily remove the line-collection artifacts, producing a DEM surface whereon cal-

culated slope and aspect are more realistic, without reducing the detail of the DEM and with modifications of the original elevations that are smaller than the LMAs of the original TRIM data. Nonetheless, the algorithm introduced a small but significant bias in the elevation measures. This could indicate that the improved topographic description is obtained at the expense of elevation accuracy. One should therefore be wary of using its results in applications that are more dependent on the elevation values than they are on the shape of the land.

The algorithm implementation is possible because the TRIM data structure preserved the original photogrammetric information as well as the entry order of the elevation points. These results clearly indicate that spatial data should be processed as little as possible by the agencies that collect it, in

TABLE 4. AREAS (Ha) OF MAP SHEETS 94B.020 AND 94B.060 FALLING IN EACH ASPECT CLASS WHEN ASPECT IS CALCULATED FROM THE ORIGINAL AND THE CROSS-SMOOTHED DEM WITH WINDOW SIZES OF 3 BY 3 AND 5 BY 5. THE ORIGINAL DEMS HAVE LOWER AREA IN THE NORTH AND SOUTH ASPECT CLASSES THAN DO THE CROSS-SMOOTHED ONES

Aspect (Azimuth)	94B.020				94B.060			
	3 by 3 Window		5 by 5 Window		3 by 3 Window		5 by 5 Window	
	Original	Cross-Smoothed	Original	Cross-Smoothed	Original	Cross-Smoothed	Original	Cross-Smoothed
No Aspect	120.2	47.9	46.0	27.0	29.8	18.0	14.9	0.0
N (337.5–22.5)	985.4	1020.2	973.5	988.6	1375.4	1642.0	1500.2	1667.0
NE (22.5–67.5)	2204.8	2485.0	2340.5	2572.6	1692.4	1787.7	1745.1	1833.3
E (67.5–112.5)	4569.0	4575.9	4695.3	4722.0	2196.3	2006.9	2053.8	1940.1
SE (112.5–157.5)	1761.3	1956.1	1812.3	1962.2	1593.4	1571.1	1648.0	1663.7
S (157.5–202.5)	932.3	1048.9	931.3	1001.7	1741.5	2017.1	1835.4	2002.8
SW (202.5–247.5)	800.7	678.6	768.8	645.9	1724.8	1695.1	1797.6	1735.0
W (247.5–292.5)	892.1	586.1	744.7	538.2	1403.5	1130.2	1217.0	1064.4
NW (292.5–337.5)	766.1	633.3	719.5	573.8	1274.9	1163.9	1219.9	1125.5



order that production artifact uncertainties can be removed using algorithms such as the one outlined in this paper.

Acknowledgments

Figures and analysis for mapsheets 94B.020 and 94B.060 are based on TRIM data produced by the Base Mapping and Geomatic Services Branch, Ministry of Sustainable Resource Management, Province of British Columbia. The TRIM data were provided to us by the Fort St. John Forest District, British Columbia Ministry of Forests, in the context of a research project funded by Forest Renewal BC. Hamish Kimmins, David Andison, Sarah McLean, and three anonymous referees provided comments that substantially improved the manuscript. Funding to Marco Albani from the University Graduate Fellowship of the University of British Columbia and the Edward W. Bassett Memorial Scholarship in Reforestation is gratefully acknowledged.

References

- Akima, H., 1978. A method of bivariate interpolation and smooth surface fitting for irregularly distributed data points, *ACM Transactions on Mathematical Software*, 4:148–164.
- Beckingham, J.D., I.G.W. Corns, and J.H. Archibald, 1996. *Field Guide to Ecosites of West-Central Alberta*, Special Report 9, Canadian Forest Service, Northwest Region, Northern Forestry Center, Edmonton, Alberta, Canada, 540 p.
- Bolstad, P.V., and T. Stowe, 1994. An evaluation of DEM accuracy: Elevation, slope, and aspect, *Photogrammetric Engineering & Remote Sensing*, 60(11):1327–1332.
- Brown, D.G., and T.J. Bara, 1994. Recognition and reduction of systematic error in elevation and derivative surfaces from 71/2-minute DEMs, *Photogrammetric Engineering & Remote Sensing*, 60(2):189–194.
- Brunson, E.G., and R.W. Olsen, 1978. Data Digital Elevation Model collection systems. *Proceedings of the Digital Terrain Models (DTM) Symposium*, 09–11 May, St. Louis, Missouri, (American Society of Photogrammetry, Falls Church, Virginia), pp. 72–99.
- Carrara, A., G. Bitelli, and R. Carlá, 1997. Comparison of techniques for generating digital terrain models from contour lines, *International Journal of Geographical Information Science*, 11(5):451–473.
- Crippen, R.E., 1989. A simple spatial filtering routine for the cosmetic removal of scan-line noise from Landsat TM P-Tape imagery, *Photogrammetric Engineering & Remote Sensing*, 55(3): 327–331.
- Evans, I.S., 1980. An integrated system of terrain analysis and slope mapping, *Zeitschrift für Geomorphologic*, Suppl-Bd 36, pp. 274–295.
- Fisher, P., 1998. Improved modeling of elevation error with geostatistics, *GeoInformatica*, 2(3):215–233.
- Fisher, P.F., 1991. First experiments in viewshed uncertainty: the accuracy of the viewshed area, *Photogrammetric Engineering & Remote Sensing*, 57(10):1321–1327.
- Florinsky, I.V., 1998. Accuracy of local topographic variables derived from digital elevation models, *International Journal of Geographical Information Science*, 12(1):47–61.
- Garbrecht, J., and P. Starks, 1995. Note on the use of USGS Level 1 7.5-Minute DEM coverages for landscape drainage analysis, *Photogrammetric Engineering & Remote Sensing*, 61(5):519–522.
- Garbrecht, J., and L.W. Martz, 2000. Digital elevation model issues in water resources modeling. *Hydrology and Hydraulic Modeling Support with Geographic Information System* (D. Maidment and D. Djokic, editors), ESRI Press, Redlands, California, pp. 1–28.
- GDBC, 1992. Digital Baseline Mapping at 1:20 000, *British Columbia Specifications and Guidelines for Geomatics*, Content Series Volume 3, Geographic Data BC, Victoria, BC, Canada, 310 p.
- , 1999. *Terrain Resource Information Management Program*, Geographic Data BC, Victoria, British Columbia URL: http://home.gdbc.gov.bc.ca/TRIM/trim/trim_overview/default.htm. (last accessed: 04 October 2002).
- Guth, P.L., 1992. Spatial analysis of DEM error, *Proceedings of ASPRS/ACSM Resource Technology 92*, 03–08 August, Washington, D.C., pp. 187–196.
- , 1999. Contour line “ghosts” in USGS Level 2 DEMs, *Photogrammetric Engineering & Remote Sensing*, 65(3):289–296.
- Hassan, M.M., 1988. Filtering digital profile observations, *Photogrammetric Engineering & Remote Sensing*, 54(10):1391–1394.
- Heuvelink, G.B.M., 1998. *Error Propagation in Environmental*

- Modelling with GIS*, Taylor & Francis, London, United Kingdom, 127 p.
- Hunter, G.J., and M.F. Goodchild, 1997. Modeling the uncertainty of slope and aspect estimates derived from spatial databases, *Geographical Analysis*, 29(1):35–49.
- Jones, K.H., 1998. A comparison of two approaches to ranking algorithms used to compute hill slopes, *GeoInformatica*, 2(3): 235–256.
- Klinkenberg, B., and M.F. Goodchild, 1992. The fractal properties of topography: A comparison of methods, *Earth Surface Processes and Landforms*, 17:217–234.
- Kok, A.L., and R.M. Rangayyan, 1987. Filtering of digitally correlated Gestalt elevation data, *Photogrammetric Engineering & Remote Sensing*, 53(5):535–538.
- Lam, N.S.N., 1983. Spatial interpolation methods: A review, *American Cartographer*, 10(2):129–149.
- Lee, J., P.K. Snyder, and P.F. Fisher, 1992. Modeling the effect of data errors on feature extraction from digital elevation models, *Photogrammetric Engineering & Remote Sensing*, 58(10):1461–1467.
- Li, Z., 1988. On the measure of digital terrain model accuracy, *Photogrammetric Record*, 12(72):873–877.
- MathSoft, 2000. *S-Plus 2000 Guide to Statistics, Vol. 1*, Data Analysis Products Division, MathSoft, Seattle, Washington, 638 p.
- Monckton, C.G., 1994. An investigation into the spatial structure of error in digital elevation data, *Innovation in GIS 1* (M.F. Worboys, editor), Taylor & Francis, London, United Kingdom, pp. 201–214.
- Oimoen, M.J., 2000. An effective filter for removal of production artifacts in U.S. Geological Survey 7.5-minute digital elevation models, *Proceedings of the Fourteenth International Conference on Applied Geologic Remote Sensing*, 06–08 November, Las Vegas, Nevada (Veridian ERIM International, Ann Arbor, Michigan), pp. 311–319.
- Pan, J.-J., and C.-I. Chang, 1992. Destriping of Landsat MSS images by filtering techniques, *Photogrammetric Engineering & Remote Sensing*, 58(10):1417–1423.
- Petrie, G., 1990. Photogrammetric methods of data acquisition for terrain modelling, *Terrain Modelling in Surveying and Engineering* (G. Petrie and T.J.M. Kennie, editors), McGraw-Hill, Inc., New York, N.Y., pp. 26–48.
- Pike, R.J., 2000. Geomorphometry—Diversity in quantitative surface analysis, *Progress in Physical Geography*, 24(1):1–20.
- Skidmore, A.K., 1989. A comparison of techniques for calculating gradient and aspect from a gridded elevation model, *International Journal of Geographical Information Systems*, 3(4):323–334.
- Weibel, M., and R. Heller, 1991. Digital terrain modelling, *Geographic Information Systems: Principals and Applications* (D.J. Maguire, M.F. Goodchild, and D.W. Rhind, editors), John Wiley & Sons, Chichester, England, pp. 269–297.
- Wood, J.D., 1996. *The Geomorphological Characterisation of Digital Elevation Models*. Ph.D. Thesis, the University of Leicester, Leicester, UK URL: http://www.geog.le.ac.uk/jwo/research/dem_char/thesis/index.html (last date accessed: 4 October 2002).

(Received 15 March 2002; revised and accepted 27 September 2002)